Thermal, Mechanical, and Morphological Analyses of Poly(2,6-dimethyl-1,4-phenylene oxide)/Styrene-Butadiene-Styrene Blends

P. S. Tucker, J. W. Barlow, and D. R. Paul*

Department of Chemical Engineering and Center for Polymer Research, University of Texas at Austin, Austin, Texas 78712. *Received October 28, 1987; Revised Manuscript Received December 30, 1987*

ABSTRACT: Blends of a styrene-butadiene-styrene, SBS, triblock copolymer with a poly(2,6-dimethyl-1,4-phenylene oxide), PPO, appear to form a single, mixed hard phase on the basis of the observation of a single, glass transition, by both differential scanning calorimetry and dynamic mechanical behavior, that varies with composition from that of polystyrene domains to that of pure PPO. The glass transition region for this phase is unusually broad, and this is believed to be caused by concentration gradients of the two types of polymer segments across the domains. Scanning transmission electron microscopy shows that the dimensions of the hard domains increase in a manner consistent with their being isotropically swollen by the PPO added. At very high PPO levels, there appears to be small quantities of an unmixed PPO phase for which no thermal transition could be detected within the limits of the techniques used. For many of the blends, the rubber and the hard phases form co-continuous networks in which the glassy phase has a spongelike form and the rubbery phase has a skeletal form. The modulus at 25 °C varies with the proportions of these phases in a manner consistent with the morphologies seen.

Introduction

Appropriately designed triblock copolymers of the styrene-butadiene-styrene, or SBS, type phase separate to give materials that behave as thermoplastic elastomers.[1-4] A great deal of research has been concerned with blending homopolymer polystyrene, PS, with such block copolymers and the question of whether the homopolymer mixes with the end-block domains or forms separate phases.[5-10] In these blends, the mixing of interest can be driven only by a small gain in combinatorial entropy but is opposed by other physical constraints.[11,12] As a result, it has been found that homopolymers must generally have molecular weights less than those of the corresponding copolymer blocks to form a mixed polystyrene phase.[5-8] When mixing does occur, there is an increase in the hard-phase volume in which the end blocks reside without any significant change in its softening point. On the other hand, addition of a different polymer having a higher glass transition temperature, T_g, than polystyrene could raise the softening point of the hard phase and extend the upper end of the temperature range for thermoplastic elastomer type behavior.

Since poly(2,6-dimethyl-1,4-phenylene oxide), PPO, is miscible with PS,[13-16] it is a candidate for blending with the SBS type copolymer to realize an increased T_g of the hard phase. The basis for miscibility of PS and PPO is an exothermic heat of mixing,[17] which introduces a new driving force for mixing with the styrene blocks of SBS that does not exist in the case of PS homopolymer. The literature contains some reports[18-20] on blends of PPO with styrene-based block copolymers that indicate substantial mixing of this polymer with the styrene blocks. However, these previous studies do not address to what extent the restrictions on homopolymer and copolymer block molecular weights for achieving miscibility are changed because of the energetic attraction between PPO and PS units. A research program focused on this issue has been initiated.[21] Some preliminary thermal analysis results were reported in an earlier paper for three different commercially available block copolymers.[22] The purpose here is to present new dynamic mechanical property and transmission electron microscopy observations for blends with PPO and one of these block copolymers. In this and the previous work a single PPO sample has been used. Future publications will deal with experimental PPO and block copolymers covering a broad range of molecular weight characteristics for each that will allow mapping of the regions of chain lengths where extensive mixing can and cannot occur.

Materials and Experimental Procedures

The poly(phenylene oxide) used here was from the same sample employed in our previous paper.[22] This material was generously donated by Dr. Joseph C. Golba, Jr., of the General Electric Co., who also supplied characterization information: $\bar{M}_n$ = 22 600, $\bar{M}_w$ = 34 000, $\bar{M}_z$ = 57 200 (by light scattering gel permeation chromagraphy), and $[\eta]$ = 0.525 dL/g (in chloroform at 25 °C).

The styrene-butadiene-styrene triblock copolymer used is a commercial product of the Shell Chemical Co. and was made available to us by G. Holden. This material, Kraton D1101, has been estimated to contain about 28.8% styrene by weight in the form of end blocks of 14 500 molecular weight each[20] that aggregate to form a dispersed glassy phase in the neat copolymer. A diffuse interface between phase domains is expected,[23-25] and the interphase for this particular copolymer may amount to as much as 24% of the total volume.[26]

The PPO and SBS were weighed in the desired proportions and added to a 3 to 1 mixture by weight of toluene and chloroform to produce a solution containing 5 wt % total polymer. The mixture was heated to about 40 °C and then precipitated into an excess of methanol at the same temperature. At this temperature, all solutions were completely clear. The precipitates were filtered and then dried in a vacuum oven for a minimum of 2 days at 60 °C. Solvent removal was essentially complete since the glass transition temperatures of the pure polymers prepared in this way were the same as those of the as received materials. Also, repeated thermal scans for blends showed no significant change in T_g. It has been noted[22] for blends of this type that no difference in glass transition behavior can be detected by using differential scanning calorimetry, DSC, for mixtures prepared by melt mixing, solvent casting, or precipitation.

Aluminum sample pans were filled (10-20 mg) with the dried precipitate of each blend and sealed for testing by a Perkin-Elmer DSC 2 equipped with a thermal analysis data station. Base-line subtraction improved the quality of the thermograms and facilitated interpretation. Results of the first thermal scan were discarded because of poor reproducibility stemming from variation in sample history. Data were collected from the second and third scans during heating and cooling at 40 °C/min. This scanning rate was chosen to increase the sensitivity of the output as described previously.[22] The glass transition temperature was taken as the mean of the onset and end-point temperatures defined by

0024-9297/88/2221-1678$01.50/0

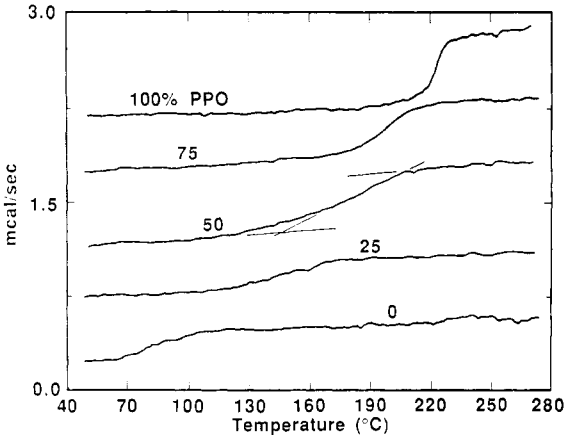

Figure 1. Representative DSC thermograms for the hard-phase transition region of the SBS/PPO blend system for mixtures containing various weight percent PPO (based on total sample mass).

the intersections of the tangents through the base lines below and above the transition and the tangent through the inflection of the transition. The breadth of the transition, ΔT_g, is equal to the end-point temperature minus the onset temperature. While thermoplastic elastomers charactersitically have glass transitions associated with both rubbery and glassy phases, only the glassy or hard-phase transition range was examined by DSC since the point of interest concerns the phase behavior of the PPO and the PS.

Samples for dynamic mechanical analysis were prepared by compression molding the precipitated powder in a special mold that prevented gross flow and, therefore, minimized sample orientation. Birefringence and simple examination of the samples revealed that anisotropy was not completely avoided. Molding temperatures ranged from 220 to 290 °C depending on PPO content. Final compression molded samples, approximately 0.15 cm thick, 1.0 cm wide, and 3–4 cm long, were tested by using a Polymer Laboratories dynamic mechanical thermal analyzer, DMTA, at a frequency of 1 Hz, a heating rate of 4 °C/min, and a deflection of 32 μm in the dual-cantilever bending mode. The glass transition temperature reported was taken as the point were the tan δ output was maximum, and modulus values discussed later are those of the real or storage modulus, E', at 25 °C.

Portions of the same compression molded samples were prepared for viewing by scanning transmission electron microscopy, STEM. Specimens were mounted, trimmed, and then sectioned to about 800 Å with an LBK ultramicrotome at cryogenic temperatures. The sections were transferred to a copper mesh grid and stained for 24 h in osmium tetraoxide vapor. Scanning transmission electron micrographs were taken on a JEOL 100CX TEM at an accelerating voltage of 100 kV and magnifications of 10 000, 20 000, 50 000, and 100 000.

Results and Discussion

Data obtained by three different techniques are presented in this section for a particular PPO/SBS blend system. The differential scanning calorimetry focused only on the high-temperature region from the T_g for PS to that of PPO. The dynamic mechanical measurements spanned a broader temperature range from which information about the low-temperature rubber T_g and the hard-phase transition behavior can be gained. Finally, transmission electron microscopy results are presented to compliment the DSC and dynamic mechanical analyses and to gain a better understanding of the blend morphology for this system.

Differential Scanning Calorimetry. Representative thermograms for the hard-phase transition region of this PPO/SBS blend system are shown in Figure 1. Thermogram interpretation is illustrated by the base line and tangent constructions shown for the blend containing 50% copolymer by weight. The hard-phase glass transition

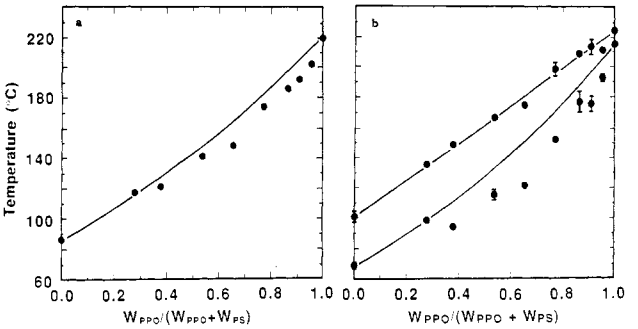

Figure 2. Glass transition behavior of PPO/SBS blends determined by DSC at 40 °C/min. Each point is an average of several determinations. Composition is expressed as mass fraction of PPO excluding the rubbery midblock. Part a shows midpoint transition values as defined in text. Part b shows the onset and end-point temperatures of the transition region (bars indicate standard deviation of several determinations; no bar indicates a small standard deviation). Solid lines in part a and the lower portion of part b were calculated from the Fox equation.

behavior for this system is summarized in Figure 2. Midpoint transition temperatures, as defined earlier, are shown in Figure 2a, while Figure 2b shows the onsets and end points of the glass transition region. The data points represent averages over several determinations for each composition. The bars in Figure 2b represent the standard deviation about the average values. The abscissa for each plot is blend composition on a rubber-free basis since this allows the data to be compared with those for PPO and PS homopolymer blends. Consistent with the findings of others,[27-29] the T_g for the polystyrene phase in the pure block copolymer (Figure 2a) is below what would be expected for pure polystyrene, PS. This has been attributed to the relatively low molecular weight of PS in the copolymer, the diffuse interphase between the component domains and surface energy effects.[27,30,31] The solid line connecting the T_g of the PS phase with the T_g of pure PPO is that calculated from the Fox equation[32] and is shown for comparison since the transition behavior of PPO blends with homopolystyrene is accurately described by this relation. The experimental data in Figure 2a show only one hard-phase T_g, indicating that the PPO and the PS are incorporated into a single phase with a T_g intermediate between that of PPO and that of the PS domains in the block copolymer. In general, the observed T_g follows closely the Fox prediction except at high PPO contents, where the data fall somewhat below the calculated line. Similar results were noted in our previous paper[22] and by Shultz and Beach[20] in their thermal optical analysis, TOA, of a similar system. The latter authors attributed the depression of the T_g from the expected results to thermal degradation during processing and scanning.

The difference between the end-point and the onset temperatures of the glass transition region serve as a measure of the transition breadth. It is somewhat instructive to examine the end-point and onset temperatures themselves (see Figure 2b) rather than just their difference. The trend of the end-point temperatures versus composition is adequately described by a straight line as shown in the upper part of Figure 2b. Only the blend containing the highest PPO content deviates visibly from the line. This deviation seems to be somewhat, but not much, greater than the experimental uncertainty. The onset temperature data are quite curved, falling well below a straight line or the Fox equation connecting the composition extremes as seen in the lower part of Figure 2b.

The breadth of the glass transition region, ΔT_g, has been associated with the intimacy of mixing of miscible blends[33]

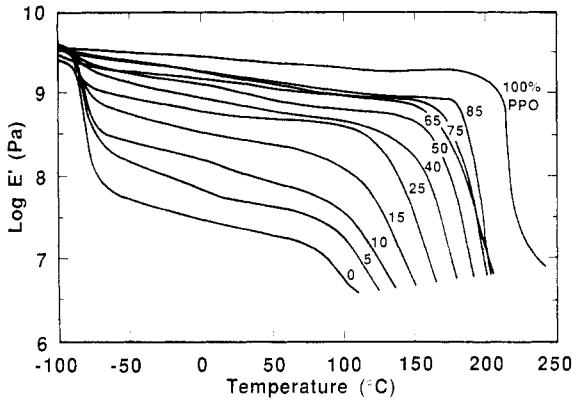

Figure 3. Storage modulus at 1 Hz for PPO–SBS blends as a function of temperature and composition (weight percent PPO of total mass). Data shown are representative of several determinations.

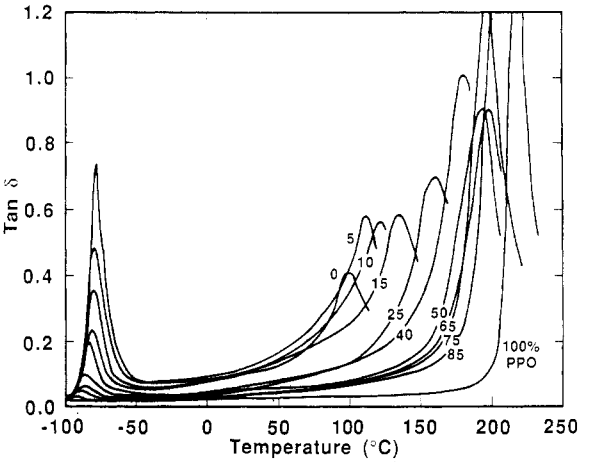

Figure 4. tan δ behavior for materials described in Figure 3.

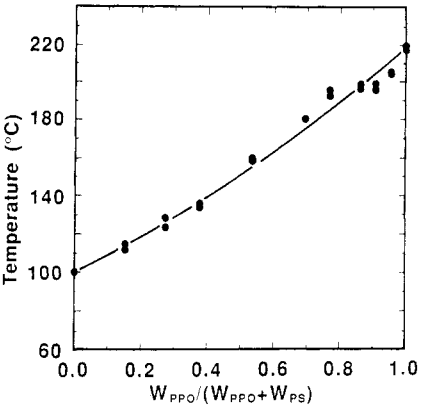

Figure 5. Temperature at which tan δ shows maximum in hard-phase transition region as a function of PPO fraction in hard phase. Data points taken from Figure 4 (other data not shown). Solid line calculated by Fox equation.

and may reflect thermodynamic composition fluctuations or longer range concentration gradients.[34] The difference between the average onset and end-point values in Figure 2b gives an average ΔT_g for each composition of the mixed PPO/PS phase. The breadth observed here for the pure PPO is consistent with other reported values.[35] Our ΔT_g for the PS phase of the SBS is also consistent with previous values for styrenic block copolymers,[27] although it is much larger than that for homopolymer PS. For the blends, ΔT_g is in all cases larger than expected by a linear additivity rule and is greater than that for the PPO/homopolymer PS blend system. Miscible homopolymers often display some increase in the breadth of the transition, which has been attributed to concentration fluctuations.[33] This extra breadth seen here may be attributed to longer range concentration gradients over distances comparable to the domain dimensions that we believe exist in addition to very local concentration fluctuations. Further evidence is apparent in the DSC thermograms themselves. As seen in Figure 1, the slope of the PS transition in the pure SBS is more shallow than the slope of the transition for pure PPO. The traces for the blends show the transition slope is most shallow near the onset, indicating PS characteristics, and becomes steeper near the end point of the transition, more indicative of PPO characteristics.

Two conclusions are apparent from the DSC examination of the SBS/PPO system. First, there appears to be one hard phase composed of PS blocks of the copolymer and the PPO homopolymer for all compositions of the blend. Second, this mixed phase of PS end blocks and PPO has a broader glass transition region than seen for homopolystyrene/PPO blends, which suggests significant concentration gradients in these domains.

Dynamic Mechanical Properties. The dynamic mechanical behavior for various SBS/PPO blends is shown in Figures 3 and 4 as a function of temperature. For the pure block copolymer, there is a large decrease in modulus at the glass transition of the rubbery phase and a corresponding peak in tan δ followed by a further decrease in modulus and another peak in tan δ at the glass transition associated with the phase formed by the polystyrene end blocks. As PPO is added, the changes in modulus and tan δ associated with rubbery phase transition occur at roughly the same temperature as for pure SBS but decrease in magnitude as should be expected. In contrast, the changes in modulus and tan δ associated with the hard-phase transition become larger and shift progressively to higher temperatures as PPO is added. That these changes seem to occur over a single temperature interval suggests there is a single hard phase composed of a mixture of the polystyrene segments and the PPO. The results shown in Figures 3 and 4 are examined in more detail in the following. The temperature at which tan δ exhibits a maximum is used as an indicator of the glass transition.

Figure 5 shows the single transition observed for the hard phase of the blends as a function of PPO mass content on a polybutadiene-free basis as before, i.e., $w_{PPO}/(w_{PPO} + w_{PS})$. The solid line was calculated from the Fox equation[32] by using the two extreme points and is shown for reference. The data generally follow the trend of the Fox predication except at higher PPO contents, where the T_g is first above the prediction and then below at the highest PPO contents, the latter being similar to what was found by DSC (Figure 2) and by thermal optical methods.[20,22] The choice of the tan δ peak to describe the T_g of the blends may have some bearing on this; however, the lack of clearly defined peaks in E'' for blends made interpretation by this method difficult and uncertain. Previous studies[36,37] have described sigmoidal shaped T_g–composition curves for miscible blends. Such a trend might describe the current results; however, beyond about 80% PPO the observed glass transition temperatures fall below the Fox prediction or any sigmoidal curve. These deviations suggest the possibility of an additional hard phase differing in PPO content; however, additional DMTA runs made in both bending and shear modes on several samples in this composition region failed to produce evidence for other transitions at temperatures higher than or lower than those shown in Figure 5.

The tan δ peaks for the hard phase of the blends are consistently broader than those for SBS or for PPO; however, this broadening does not seem to be as exag-

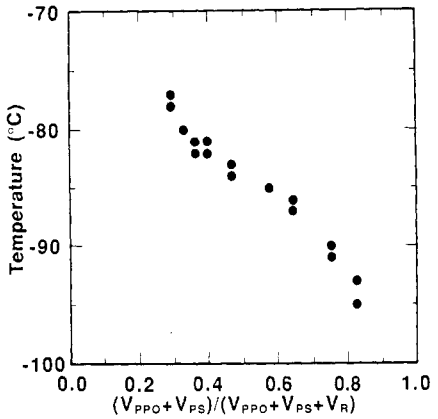

Figure 6. Temperature at which tan δ shown maximum in rubber phase transition region as a function of volume fraction of hard phase.

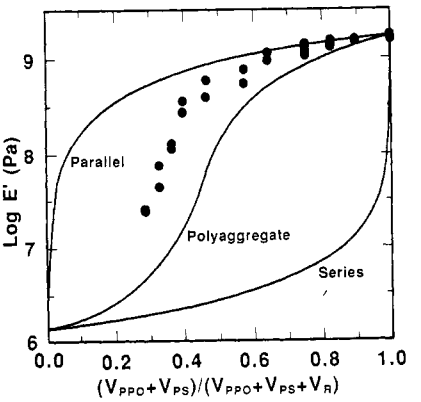

Figure 7. Storage modulus at 25 °C as a function of hard-phase volume fraction (dots). Solid lines calculated from parallel, series, and Kerner's polyaggregate models for composites of hard and soft phases.

gerated as that indicated by the DSC results. Similar comparisons have been made between mechanical and thermal analysis of simple miscible blend systems.[38]

A closer examination of the tan δ peak for the rubbery phase reveals that its maximum shifts slightly to lower temperatures as PPO is added (see Figure 6). Others[39] have noted a similar phenomenon for rubber dispersed in a glassy phase. Bates et al.[40] report a lowering of the rubber phase T_g for a series of block copolymers in which the polybutadiene molecular weight increased while maintaining a constant morphology. They argued rather convincingly that this was the result of stresses created by the difference in thermal expansion coefficients of the soft and hard phases. A similar effect may explain the results shown in Figure 6.

Practical interests in triblock copolymers, such as the SBS type, stem primarily from their thermoplastic elastomer characteristics. One feature of this behavior is the relatively temperature-independent modulus in the vicinity of the use temperature with the upper and lower limits of this region being defined by the softening temperatures of the two phases. The absolute value of this plateau modulus is governed by the relative proportions of the two phases and their spatial arrangement or morphology. As seen in Figure 3, the upper temperature limit of this region can be significantly extended by addition of PPO if it mixes with the hard-phase segments of the block copolymer. However, addition of PPO also increases the plateau modulus since the fraction of the hard phase is increased. Changes in morphology may also affect how the modulus responds to addition of PPO. Modulus values at 25 °C from Figure 3 are plotted in Figure 7 versus the total hard-phase fraction of the blends. The value at 29% hard phase is that of the pure SBS where the hard phase is entirely polystyrene. The solid curves represent idealized models for two phase systems of a rubbery and a hard, glassy material. The upper curve displays the behavior of a parallel arrangement,[41] while the lower curve represents a series arrangement.[41] The hard-phase properties are dominant as expected for the former case, and the rubbery phase properties are dominant for the latter. This behavior is similar to that expected for a dispersed rubber phase and a dispersed glassy phase, respectively. The sigmoidal-shaped curve represents the Kerner polyaggregate or packed grain model,[42] which assumes two dissimilar phases are randomly dispersed in a third matrix phase as the volume fraction of the latter tends to zero. Of the many available models, this one was chosen for comparison, since it accurately describes the modulus–composition behavior of styrene–butadiene triblock copolymers prepared in a similar manner.[43]

Values of the modulus for the polybutadiene and the polystyrene phases of the copolymer cannot be measured directly, but estimates can be readily obtained from the literature.[43,44] The moduli for pure PPO and pure PS differ by approximately 10%, and some blend compositions have values that are greater than those of either pure component.[45] However, when transferred to the logarithmic scale of Figure 7, such differences are not detectable. For simplicity, we have considered the mixed phase of PPO and PS to have a constant modulus regardless of its composition. This should be of little consequence considering the magnitude of the modulus difference between the glassy and rubbery phases.

The data points in Figure 7 appear to follow the general shape of the polyaggregate model although they are shifted to the left considerably. It is reasonable to conclude from Figure 7 that the rubber behaves essentially as a dispersed phase at high PPO content. Below about 70% hard phase, a more complex morphology is likely. The measured modulus is considerably higher than predicted by the polyaggregate model. Relative to this model, the glassy phase behaves as if it has a higher volume fraction than is actually present in the blend. One possible explanation is that the connectivity of the glassy phase is greater than expected from the polyaggregate model, approaching that of a true matrix phase, although both phases could still be co-continuous. According to the Kerner's model, each phase contributes equally to the spatial arrangement. Allowing the rubbery phase to become more convex (like a dispersed phase) and the glassy phase to become more concave (like a matrix phase) at a fixed volume fraction would result in a composite with a higher modulus because of the increased connectivity of the glassy phase. For samples involving flow during formation, it has been demonstrated for extrusions of block copolymers[46,47] that the hard-phase connectivity is higher in the direction of flow (tangential) than in the normal direction, so the modulus may be greater in the test direction than in the normal or thickness direction. Electron micrographs, presented in the next section, support a co-continuous structure with a matrixlike glassy phase.

Electron Microscopy. The phase morphology of these materials was examined by scanning transmission electron microscopy with OsO_4 to stain the phase formed by the unsaturated midblock. In the photomicrographs shown here this phase appears dark, while the hard phase should be light since it is not expected to be stained.

Figure 8 shows the structure of the pure SBS. The dark phase is clearly the continuous one, while the light phase

Figure 8. STEM photomicrograph of SBS block copolymer. Sample prepared by precipitation from solution then compression molding of precipitate. Thin sections exposed to OsO_4 vapor to yield dark rubber phase.

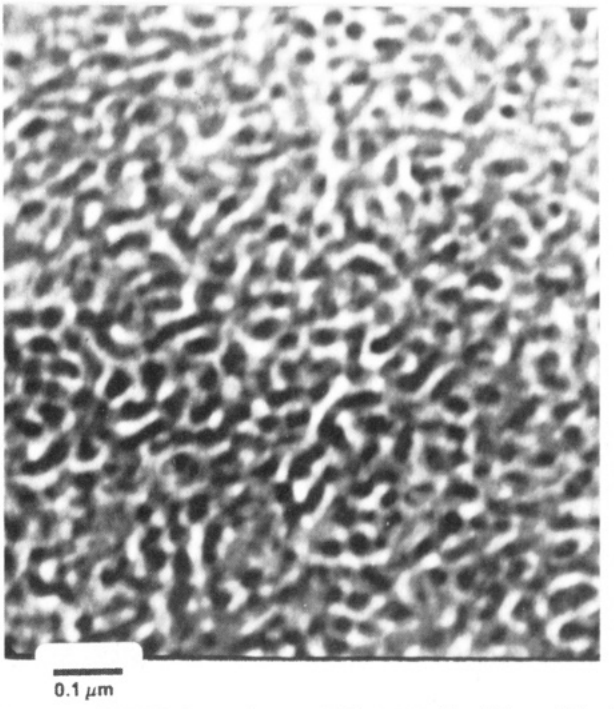

Figure 9. STEM photomicrograph for 50:50 blend by weight of SBS and PPO prepared in the same manner as Figure 8. Note that glassy domains (light) are larger than in Figure 8 and appear to be continuous.

is dispersed but has shapes that are somewhat ambiguous to interpret. On the basis of all information available, the hard phase is probably in the form of rods, although the presence of some spheres or lamellae cannot be ruled out from the micrograph alone. On the basis of a random statistical analysis of this micrograph, the average *minimum* characteristic dimension of the dispersed light phase is 140 Å. The predicted dimension for polystyrene segments of this molecular weight assuming a spherical morphology is 125 Å.[48] Figure 9 is a photomicrograph for a 50/50 blend by weight of PPO and SBS corresponding to 65% (by weight) of hard phase and 35% rubber. From simple inspection, it is clear that the light or hard phase is continuous and mostly concave in shape. The dark or rubbery phase, on the other hand, has more convex features. In this two-dimensional view, this phase appears to have both continuous and disperse characteristics; however, a spongelike network is probably a more apt description of the total morphology. Gergen et al.[26] have described similar morphologies that they refer to as "skeletal-matrix" structures.

While both are continuous, the "skeletal" phase could be construed as more typical of a dispersed phase by its convex features, and the "matrix" phase would be more like a true matrix in which the features are generally concave with greater connectivity. The properties then would be dominated somewhat more by the concave phase. The modulus–composition behavior presented previously indicates that the hard-phase properties dominate relative to the case where both phases contribute equally to the spatial arrangement, i.e., the polyaggregate model. This spongelike morphology seen in the photomicrographs is consistent with the modulus behavior for these blends.

From comparison of Figures 8 and 9, it is clear that the average dimension of the light phase has increased by addition of PPO, which is consistent with it forming a mixed phase with the polystyrene segments. Figure 10 shows how the average *minimum* characteristic dimension of the light or hard phase increases with amount of PPO

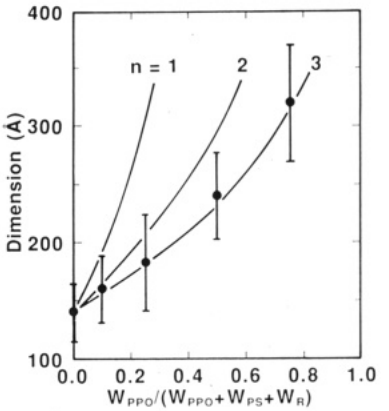

Figure 10. Average minimum characteristic dimension (dots) of glassy phase obtained from analysis of STEM photomicrographs. Bars indicate range. Lines represent calculations via eq 1 for swelling of this phase in one direction ($n = 1$), two directions ($n = 2$), and three directions ($n = 3$). Subscript R denotes rubber.

added. These results represent a statistical analysis of several micrographs at each composition, and the bars indicate the standard deviation for 30 measurements. Three theoretical lines designated as $n = 1$, 2, and 3 are shown that were calculated as follows:

$$\frac{d}{d_0} = \left(\frac{w_{PS} + w_{PPO}}{w_{PS}} \right)^{1/n} \tag{1}$$

where d is the hard-phase dimension for the blend and d_0 is the corresponding quantity for pure SBS. Since the density of PPO and PS are nearly identical, the use of weight rather than volume in eq 1 presents no problem. This equation assumes that all of the PPO adds to the PS domains and that the corresponding swelling occurs only in one direction when $n = 1$, equally in two directions when $n = 2$, or isotropically in all three directions when $n = 3$. A simple physical way to think of these various cases is spheres that grow in radius ($n = 3$), rods that grow only

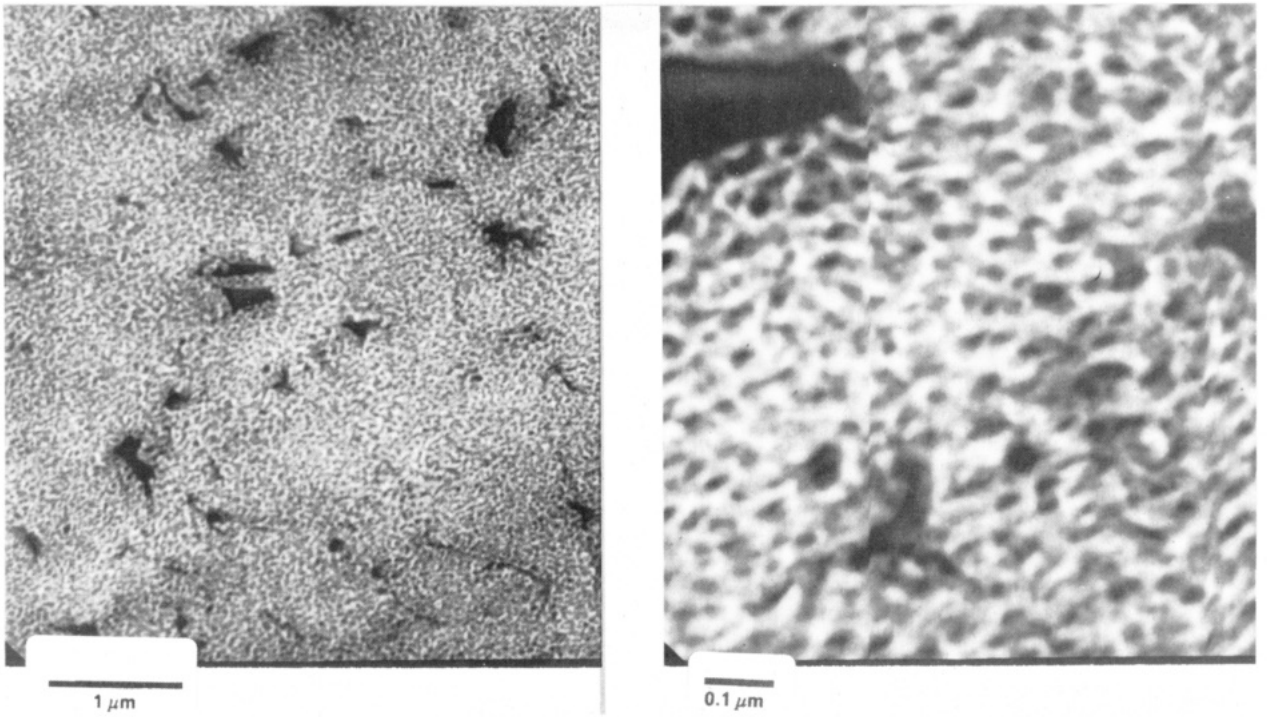

Figure 11. STEM photomicrograph for 25:75 blend by weight of SBS and PPO prepared as in Figure 8. Note the few large irregular, dark domains dispersed throughout, which are not seen in Figures 8 and 9.

in radius (n = 2), or lamellae that grow only in thickness (n = 1). However, rods and lamellae may also swell isotropically in all three directions as well. The results in Figure 10 agree very well with n = 3 (setting d_0 = 140 Å), which indicates that the hard phase swells isotropically in all three directions regardless of the shape of this phase and that essentially all of the PPO is accounted for by the calculation.

Blends containing 75% PPO and 25% SBS (or 82% hard phase and 18% rubber) contain a morphological feature not seen at lower PPO contents. Figure 11 shows two photomicrographs of different magnifications. The bulk of the field of view consists of the same spongelike, co-continuous structure described earlier, but in addition there are a few large (about 1000 Å), irregularly shaped particles dispersed throughout. Since the particles are very dark, the visual evidence would suggest that they are rich in butadiene segments because these are the only units present normally expected to be stained by OsO_4.[49] However, there is no evidence for polystyrene domains within the particles, so it seems unlikely that they could be regions of unmixed SBS. Because the particles are much larger than the dimensions of the midblock (end-to-end distance 220 Å) they cannot reasonably be interpreted as a pure polybutadiene phase with the PS end blocks outside their borders. Physically one could believe they are composed of PPO that did not mix with the PS end blocks for either kinetic or equilibrium reasons. Some of the earlier results can be construed as consistent with such a hypothesis. Recall that for this composition, the hard-phase T_g from both DSC and DMTA falls slightly below the value expected from the prediction by the Fox equation[32] as seen in Figures 2 and 5. The T_g depression is consistent with not all of the PPO being mixed with the PS end blocks, and it is possible that an extra PPO phase could not be detected by DSC or DMTA despite our repeated efforts to find a transition for such a phase. The problem with this hypothesis is that there is no direct evidence in the literature that suggests PPO can be stained by OsO_4. Our own electron micrographs of sections of pure PPO that had been exposed to OsO_4 were inconclusive since the material is uniform and adjustment of the contrast in STEM can make what is seen appear very dark or very light. However, when bulk PPO is exposed to OsO_4 vapor, the material, by visual inspection, becomes very dark as does the unsaturated rubber. Scraping the darkened PPO surface did not uncover a lighter material underneath. The literature[50] does suggest that OsO_4 reacts with moieties, e.g., –OH, –NH2 and –O–, other than just double bonds. The higher reactivity of the double bonds would, of course, cause a rubber-stained phase to appear darker than a PPO-stained phase. In Figure 11, the irregular phases are large enough to extend through the thickness of the section. Even if the PPO is only slightly stained, the mass thickness would cause this phase to appear quite dark. At the same time, the small, spherical particles, presumed to be polybutadiene, are so small relative to the section thickness that the contrast normally expected would be diluted by the mixed, glassy phase above and below the particles. In this case, both the large, irregular domains and the small, spherical domains could easily appear to be of similar contrast. Thus, we feel that our hypothesis of PPO particles in Figure 11 is viable but not completely proven. One would expect that the interface of these larger domains consists of a mixed PPO–PS end-block phase, although it cannot be directly observed in these micrographs.

Summary

Because of the significant difference in the T_g values for PPO and PS, examination of glass transition behavior is a useful way to investigate the extent to which the homopolymer mixes with the styrene blocks of an SBS copolymer. Both the thermal and dynamic mechanical results given here suggest that within the limits of detection there is a single, composition dependent T_g for the nonrubbery portion of blends of the particular PPO and SBS polymers used. The same conclusion has been reached previously by using similar materials.[20,22] However, at high PPO content in these blends, electron microscopy indicates

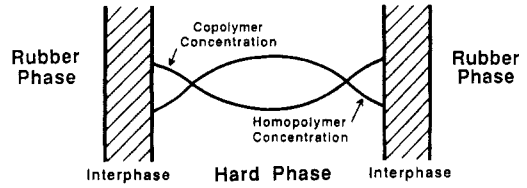

Figure 12. Illustration of gradients of PPO and PS segment concentrations in mixed hard domain.

the presence of small amounts of an additional phase that we identify tentatively as essentially pure PPO. While we cannot be sure that this phase is an equilibrium feature of the mixture, its presence is qualitatively consistent with statistical thermodynamic theories of Meier[51] and Hong and Noolandi[52] that predict a homogeneous homopolymer phase in equilibrium with the mixed mesophase on this end of the composition scale. Apparently the DSC and DMTA were not able to detect this phase, probably owing to its low content; but an additional phase is consistent with the lower T_g found than expected by both techniques. This T_g anomaly is also evident in the results presented earlier by Shultz and Beach[20] using a thermal optical technique.

Aside from the exception noted above, the PPO and SBS used here form blends with a single hard phase that grows in dimension as PPO is added. The relationship between the minimum characteristic phase dimension and PPO content is consistent with isotropic swelling of the hard phase, regardless of its shape, by the addition of PPO.

At low PPO contents, the hard phase has primarily convex surfaces and might be described as a dispersed phase, although its shapes are complex and probably do not represent equilibrium structures. At hard-phase fractions above about 70%, the modulus values, measured at 25 °C, indicate a dispersed rubbery phase in a glassy matrix. Intermediate blend compositions appear to have a co-continuous morphology in which the rubber phase appears to form and behaves as a skeletal structure throughout the spongelike, glassy phase.

Recently, Jiang et al.[53] proposed a thermodynamic model for describing blends of a block copolymer with a homopolymer having the same repeat structure as one of the blocks. They explicitly introduce the idea of a concentration gradient spanning the mixed phase composed of end blocks and homopolymer. Figure 12 presents the general features of this idea. At the interface, the concentration of end-block segments is highest and the concentration of homopolymer is lowest. In the pure copolymer, the end blocks must extend at least to the center of the domain to maintain a constant density. As homopolymer is added, the size of the mixed domain increases, so it is likely that the end-block segments can undergo some decrease in concentration from the interface to the center of the domain. The homopolymer on the other hand must be distributed in a manner preventing significant density gradients, i.e., the homopolymer concentration will be highest at the center of the domain and decrease to the interface. Substantial broadening of the T_g for this phase in this SBS/PPO system seen by DSC and DMTA beyond that noted for PPO/PoS blends supports the existence of such concentration gradients which span the dimensions of the domains.

Thomas and co-workers[54] have conclusively identified an ordered co-continuous structure for star-block copolymers known as the tetrapod or double diamond. This structure has also been observed for diblock copolymers.[54] In many cases, extensive annealing was necessary for this structure to form. For some of the compositions reported here the two phases appear to have some co-continuous character; however, the structures obtained were not highly ordered. Figure 9 displays features that might indicate a tendency for this type of ordered co-continuous structure. The glassy, light phase extends from numerous central points in three directions like spokes of a wheel—similar to Thomas's results. With the appropriate thermal treatment that would allow closer approach to equilibrium morphologies, more highly ordered structures for the present system are a possibility that deserves attention. Limited annealing studies are in progress in this laboratory.

As a final point, it should be noted that well-mixed hard phases of PPO and PS end blocks occur only when the molecular weights of these species bear an appropriate relationship with one another.[21] Future publications will deal with quantification of this issue and the role of the enthalpic driving force for mixing of the homopolymer and the segments of the appropriate copolymer block on this relationship.

Acknowledgment. We express appreciation to Phillips Petroleum Foundation for a fellowship, to General Motors Research Laboratories for partial financial support, and to S. Y. Hobbs for valuable discussions about STEM interpretation.

Registry No. PPO (copolymer), 25134-01-4; PPO (SRU), 24938-67-8.

References and Notes

(1) Beecher, J. F.; Marker, L.; Bradford, R. D.; Aggarwal, S. L. *J. Polym. Sci., Part C* **1969**, *26*, 117.
(2) Shen, M. *Adv. Chem. Ser.* **1979**, *No. 176*, 181.
(3) Riess, G.; Hurtrez, G.; Bahadur, P. In *Encyclopedia of Polymer Science and Engineering*; Kroschwitz, J. I., Ed.; Wiley: New York, 1985; Vol. 2, p 324.
(4) Holden, G.; Bishop, E. T.; Legge, N. R. *J. Polym. Sci., Part C* **1969**, *26*, 37.
(5) Aggarwal, S. L.; Livigni, R. A. *Polym. Eng. Sci.* **1977**, *17*, 498.
(6) Inoue, T.; Soen, T.; Hashimoto, T.; Kawai, H. *Macromolecules* **1980**, *3*, 87.
(7) Reiss, G.; Kohler, J.; Tournut, C.; Bandaret, A. *Makromol. Chem.* **1967**, *101*, 58.
(8) Skoulios, A.; Helffer, P.; Gallot, Y.; Selb, J. *Makromol. Chem.* **1971**, *148*, 305.
(9) Class, J. B. *Rubber Chem. Technol.* **1986**, *58*, 973.
(10) Roe, R.-J.; Zin, W. C. *Macromolecules* **1984**, *17*, 189.
(11) Meier, D. J. *Polym. Prepr. (Am. Chem. Soc., Div. Polym. Chem.)* **1977**, *18*, 340.
(12) Xie, H.; Liu, Y.; Jiang, M.; Yu, T. *Polymer* **1986**, *27*, 1928.
(13) MacKnight, W. J.; Karasz, F. E.; Fried, J. R. In *Polymer Blends*; Paul, D. R., Newman, S., Eds.; Academic: New York, 1978; Vol. 1, Chapter 5.
(14) Bair, H. E. *Polym. Eng. Sci.* **1970**, *10*, 247.
(15) Shultz, A. R.; Gendron, B. M. *J. Appl. Polym. Sci.* **1972**, *16*, 461.
(16) Fried, J. R. In *Developments in Polymer Characterization*; Dawkins, J. V., Ed.; Applied Science: London, 1982; Vol. 4, Chapter 2.
(17) Weeks, N. E.; Karasz, F. E.; MacKnight, W. J. *J. Appl. Phys.* **1977**, *48*, 4068.
(18) Kambour, R. P., to General Electric Co.; U.S. Patent 3 639 508, February 1, 1972.
(19) Hansen, D. R., to Shell Development Co.; U.S. Patent 4 141 876, Feb 26, 1979; U.S. Patent 4 104 323, Aug 1, 1978.
(20) Shultz, A. R.; Beach, B. M. *J. Appl. Polym. Sci.* **1977**, *21*, 2305.
(21) Tucker, P. S. Doctoral Dissertation, University of Texas, 1988.
(22) Tucker, P. S.; Barlow, J. W.; Paul, D. R. *J. Appl. Polym. Sci.* **1987**, *34*, 1817.
(23) Leary, D. F.; Williams, M. C. *J. Polym. Sci., Polym. Lett. Ed.* **1970**, *8*, 355; *J. Polym. Sci., Polym. Phys. Ed.* **1973**, *11*, 345.
(24) Hashimoto, T.; Fujimura, M.; Kawai, H. *Macromolecules* **1981**, *14*, 1196; **1980**, *13*, 1660; **1980**, *13*, 1237.
(25) Richards, R. W.; Thomason, J. L. *Macromolecules* **1983**, *16*, 982; *Polymer* **1983**, *24*, 1089; **1983**, *24*, 275; **1981**, *22*, 581.
(26) Gergen, W. P.; Lutz, R. G.; Davidson, S. In *Thermoplastic Elastomers Research and Development*; Legge, N. R., Holden, G., Schroeder, H., Eds.; Hanser: Munich, 1987; Chapter 14.

(27) Granger, A. T.; Wang, B.; Krause, S.; Fetters, L. J. *Adv. Chem. Ser.* **1986**, *No. 211*, 127.
(28) Krause, S.; Lu, Z.-H.; Iskandar, M. *Macromolecules* **1982**, *15*, 1076.
(29) Krause, S.; Iskandar, M. *Adv. Chem. Ser.* **1979**, *No. 176*, 205.
(30) Hashimoto, T.; Tsukahara, T.; Tachi, K.; Kawai, H. *Macromolecules* **1983**, *16*, 648.
(31) Guar, U.; Wunderlich, B. *Macromolecules* **1980**, *13*, 1618.
(32) Fox, T. G. *Bull. Am. Phys. Soc.* **1956**, *2*, 123.
(33) MacKnight, W. J.; Karasz, F. E.; Fried, J. R. In *Polymer Blends*; Paul, D. R., Newman, S., Eds.; Academic: New York, 1978; Vol. 1, Chapter 5.
(34) Keskkula, H.; Paul, D. R.; Young, P.; Stein, R. S. *J. Appl. Polym. Sci.* **1987**, *34*, 1861.
(35) Fried, J. R.; Lorenz, T.; Ramdas, A. *Polym. Eng. Sci.* **1985**, *25*, 1048.
(36) Fried, J. R.; Hanna, G. A. *Polym. Eng. Sci.* **1982**, *22*, 705.
(37) Shultz, A. R.; Beach, B. M. *Macromolecules* **1974**, *7*, 902.
(38) Fernandes, A. C. Doctoral Dissertation, University of Texas, 1986.
(39) Bohn, L. *Adv. Chem. Ser.* **1975**, *No. 142*, 66. Kraus, G.; Fodor, L. M.; Rollman, K. W. *Polym. Prepr. (Am. Chem. Soc., Div. Polym. Chem.)* **1978**, *19*, 68. Krause, S.; Wang, B. *J. Polym. Sci., Polym. Lett. Ed.* **1986**, *24*, 35.
(40) Bates, F. E.; Cohen, R. E.; Argon, A. S. *Macromolecules* **1983**, *16*, 1108.
(41) Nielsen, L. *Mechanical Properties of Polymers and Composites*; Marcel Dekker: New York, 1974; Vol. 2.
(42) Kerner, E. H. *Proc. Phys. Soc.* **1956**, *69B*, 808.
(43) Faucher, J. A. *J. Polym. Sci., Polym. Phys. Ed.* **1974**, *12*, 2153.
(44) Aggarwal, S. L. *Polymer* **1976**, *17*, 938.
(45) Kleiner, L. W.; Karasz, F. E.; MacKnight, W. J. *Polym. Eng. Sci.* **1979**, *19*, 519.
(46) Kraus, G.; Rollman, K. W.; Gardner, J. O. *J. Polym. Sci., Polym. Phys. Ed.* **1972**, *10*, 2061.
(47) Odell, J. A.; Keller, A. *Polym. Eng. Sci.* **1977**, *17*, 544.
(48) Meier, D. J. In *Block and Graft Copolymers*; Burke, J. J., Weiss, V., Eds.; Syracuse University Press: New York, 1973; Chapter 6.
(49) Kato, K. *J. Polym. Sci., Part B* **1966**, *4*, 35; *Polym. Eng. Sci.* **1967**, *7*, 38.
(50) Niinomi, M.; Katsuta, T.; Kotani, T. *J. Appl. Polym. Sci.* **1975**, *19*, 2919.
(51) Meier, D. J. *Polym. Prepr. (Am. Chem. Soc., Div. Polym. Chem.)* **1977**, *18*, 340.
(52) Noolandi, J.; Hong, K. M. *Polym. Bull.* **1982**, *7*, 561; *Macromolecules* **1983**, *16*, 1083; *Ber. Bunsen-Ges. Phys. Chem.* **1985**, *89*, 1147.
(53) Xie, H.; Liu, Y.; Jiang, M.; Yu, T. *Polymer* **1986**, *27*, 1928.
(54) Alward, D. B.; Kinning, D. J.; Handlin, D. L.; Thomas, E. L.; Fetters, L. J. *Macromolecules* **1986**, *19*, 215; **1986**, *19*, 1288; **1986**, *19*, 2197.

Solute Diffusion in Polymers. 2. Fourier Estimation of Capillary Column Inverse Gas Chromatography Data

Craig A. Pawlisch,† John R. Bric,‡ and Robert L. Laurence*

Department of Chemical Engineering, University of Massachusetts, Amherst, Massachusetts 01003. *Received October 15, 1987; Revised Manuscript Received December 17, 1987*

ABSTRACT: Moment analysis of capillary column inverse gas chromatography (IGC) data provides accurate measurement of polymer–solute diffusion coefficients. The technique is ideal for studying interactions of volatile materials with molten or rubbery polymers, at conditions approaching infinite dilution of the volatile component. The analysis presented by Pawlisch et al.,[1] however, can provide flawed results if the geometry of the column coating is not uniform or if the polymer/solute system exhibits elution curves with significant skewing. In this paper, we present two improvements that overcome these limitations: (1) a model that accounts for a nonuniform polymer film and (2) a method for parameter estimation in the Fourier domain. The usefulness of the improvements is demonstrated by measuring the diffusivity and activity of benzene, toluene, and ethylbenzene in polystyrene, between 110 and 140 °C, the system investigated in part 1, and of methanol, methyl acetate, and methyl methacrylate in poly(methyl methacrylate) at temperatures above the glass transition temperature. In addition, the IGC technique is demonstrated to be applicable at temperatures below the glass transition temperature, as successful sub-T_g measurements were made for methanol in poly(methyl methacrylate). Finally, criteria are presented for the experimental modifications necessary to reduce the skewing of elution curves, which can reduce the reliability of results.

Introduction

Inverse gas chromatography (IGC) is now well established as a means of studying interactions between polymers and volatile solutes. In a typical application, the polymer is used as the stationary phase of a chromatographic column, while a pulse of the volatile solute is vaporized and injected into a carrier gas that flows through the column. The retention time and the elution profile of the solute pulse, affected by interactions between the solute and the stationary phase, can be used to study those interactions. Because the volume of injected solute (sometimes referred to as a probe) is small (0.2 μL of liquid), interactions between the probe and the stationary phase generally occur at solute concentrations approaching infinite dilution. Depending upon the physical state of the polymer and the nature of the probe, a wide variety of physical and/or chemical properties can be measured. Reported applications of the technique include measurements of thermodynamic properties of solutions, surface sorption characteristics, phase-transition temperatures, and degree of crystallinity of the polymeric phase. These applications have been reviewed in detail by several authors.[2-5]

IGC has also been proposed as a means of studying diffusion of solutes within a polymeric material. It has long been recognized that transport limitations in the stationary phase can produce significant broadening and distortion of a chromatographic peak. A number of researchers have attempted to exploit this phenomenon as a means of measuring the diffusion coefficient of the probe substance in the stationary phase.[6-11] In all of these studies, packed

† Current address: Research Laboratories, Union Camp Corp., Princeton, NJ.
‡ Polymer Science and Engineering Department, University of Massachusetts.

0024-9297/88/2221-1685$01.50/0